

LITERATURE CITED

1. G. N. Abramovich, The Theory of Turbulent Jets [in Russian], Fizmatgiz, Moscow (1960).
2. L. A. Vulis and V. P. Kashkarov, The Theory of Jets of Viscous Liquid [in Russian], Nauka, Moscow (1965).
3. A. S. Ginevskii, The Theory of Turbulent Jets and Wakes [in Russian], Mashinostroenie, Moscow (1969).
4. O. V. Yakovlevskii, Izv. Akad. Nauk SSSR, Mekh. Mashinostr., No. 3 (1961).
5. A. Ferri, P. A. Libby and V. Zakkay, High Temperatures in Aeronautics, Pergamon Press, Milan (1964).
6. L. A. Vulis and L. P. Yarin, Fiz. Goreniya Vzryva, 10, No. 2 (1974).
7. P. O. Vittse, Raketn. Tekh. Kosmonavt., 12, No. 4 (1974).
8. G. N. Abramovich, S. Yu. Krashennnikov, A. N. Sekundov, and I. P. Smirnova, in: Turbulent Displacement of Gas Jets [in Russian] (edited by G. N. Abramovich), Nauka, Moscow (1974).
9. N. N. Terekhina, in: Investigation of the Physical Foundations of the Operation of Furnaces and Ovens [in Russian], Izd. Akad. Nauk KazSSR, Alma-Ata (1957).
10. V. Ya. Bezmenov and V. S. Borisov, Izv. Akad. Nauk SSSR, Otd. Tekh. Nauk, Mekh. Mashinostr., No. 4 (1961).
11. D. Gray and P. Jakobs, Raketn. Tekh. Kosmonavt., 2, No. 3 (1964).
12. W. K. Keagy and A. E. Weller, in: Proceedings of the 1949 Heat Transfer and Fluid Mechanics Institute, American Society of Mechanical Engineers, New York (1949).
13. J. O. Hinze and B. G. van der Heggezijnen, in: Proceedings of the Seventh International Congress on Applied Mechanics, Vol. 2, Part 1, London (1948), p. 286.
14. M. S. Uberoi and L. G. Garby, Phys. Fluids, 10, No. 9, Part 2 (1967).
15. S. Corrsin and M. Uberoi, NASA Report 998 (1950).
16. H. Ihlenfeld, Maschinenbautechnik, 22, No. 4 (1973).

INFLUENCE OF FUNDAMENTAL FORCE FACTORS ON THE TRANSVERSE VELOCITY
OF FINE PARTICLES MOVING IN A TURBULENT GAS STREAM

Z. R. Gorbis, F. E. Spokoynyi,
and R. V. Zagainova

UDC 532.582.7

On the basis of a numerical solution of the equations of fine particle motion in a turbulent vertical stream forces of a different nature, acting in the radial direction and governing the average transverse particle velocity, are analyzed.

The motion of axisymmetric streams of a gas suspension has been examined in many cases as one-dimensional [1, 2]. The magnitudes of the longitudinal velocity and the concentration have hence been considered averaged over the cross section, and the transverse particle velocity has been taken as zero. However, formation of a concentration profile, whose analysis is possible only in the presence of information about the transverse particle motion in the gas suspension stream, acquires special value for different heat- and mass-transfer processes, the deposition of particles on channel walls, etc. The appearance of a radial component of the average particle velocity is due to the presence of a number of force effects, to be considered later, which act in the transverse direction. The particle motion hence specifies the appearance of mass fluxes of a different nature: the average transverse motion is a source of convective mass transport and the pulsating motion is diffuse. The radial flux density of the particle mass is $j = \beta v_s - D_s (d\beta/dr)$. In a steady gas suspension

Odessa Technological Institute of the Refrigeration Industry. Odessa State University.
Translated from Inzhenerno-Fizicheskii Zhurnal, Vol. 30, No. 4, pp. 657-664, April, 1976.
Original article submitted June 19, 1975.

This material is protected by copyright registered in the name of Plenum Publishing Corporation, 227 West 17th Street, New York, N.Y. 10011. No part of this publication may be reproduced, stored in a retrieval system, or transmitted, in any form or by any means, electronic, mechanical, photocopying, microfilming, recording or otherwise, without written permission of the publisher. A copy of this article is available from the publisher for \$7.50.

these mechanisms cancel out and assure constancy of the concentration fields. It follows from the expression presented that under these conditions ($j = 0$), the average radial particle velocity is known not to be zero for $d\beta/dr \neq 0$. To determine the magnitude of this velocity it is necessary to use the equation of particle motion, which most completely reflects the effects of the force factors. Many such forces were noted in [3, 4]; however, even the qualitative nature of their influence remains unexplained. Attempts at a quantitative comparison of the magnitudes of the forces are presented in [5, 6], but many of these estimates are not correct in connection with the incomplete and inadequately founded selection of a number of initial dependences and parameters [1]. In the majority of other papers [7-12], only 1-2 of the possible mechanisms are taken into account and nowhere is the accessibility of neglecting the remaining factors estimated. Hence, by considering substantially analogous flow conditions, different authors consider mechanisms of different nature to be governing. A further analysis is performed on the basis of the equations of motion obtained for monodispersed fine particles (subject to Stokes law) in a vertically ascending gas suspension stream:

$$\begin{aligned} \frac{Fr}{2} \left(1 - \frac{\rho}{\rho_s} \right) + \frac{U - U_s}{2Stk} - V_s \frac{dU_s}{dR} + \frac{2}{ReR} \frac{d}{dR} \left(R Sc^{-1} \frac{dU_s}{dR} \right) = 0, \quad (1) \\ - \frac{V_s}{Stk} - V_s \frac{dV_s}{dR} + \frac{3,09}{V\sqrt{2}Re} \frac{\rho}{\rho_s} \frac{D}{d_s} \left(U_s - U - \frac{d_s}{D} \frac{dU}{dR} \right) \times \\ \times \left| \frac{dU}{dR} \right|^{1/2} + \frac{K_E}{R} \int_0^R \beta_r R dR - 9 \frac{\rho}{\rho_s} \left(\frac{D}{d_s Re} \right)^2 \left(1 - \frac{T_w}{T_0} \right) \frac{dU}{dR} + \\ + 2,25 \frac{\rho}{\rho_s} \left(\frac{D}{d_s} \right)^3 \frac{Bi_R}{Re^2} \left[1 - \left(\frac{T_w}{T_0} \right)^4 \right] f_R (Bu, \beta_r) - \frac{1}{2} \frac{d \langle V_s'^2 \rangle}{dR} = 0. \quad (2) \end{aligned}$$

Here we use the dimensionless variables $U = u/u_0$; $U_s = u_s/u_0$; $V_s = v_s/u_0$; $R = r/r_w$; $\beta_r = \beta/\beta_0$; the complexes $Fr = gD/u_0^2$; $Stk = Re\rho_s d_s^2/18\rho D^2$; $Re = u_0 D/\nu$; $Sc = \nu/D_S$; and $Bu = 0.75k_f \beta_0 D/d_s$ are the Froude, Stokes, Reynolds, Schmidt, and Bouguer criteria; $Bi_R = \sigma T_0^3 d_s/\lambda_s$ is the Biot radiation criterion; and $K_E = q^2 r_w^2 \rho_s \beta_0/\epsilon_0 u_0^2$. The members in (1) reflect the contribution of gravity, the drag force during longitudinal relative motion of the components, and the inertial force of the particles, written taking into account the average and pulsating velocities. A larger number of force factors act on the particle in the radial direction: the members in (2) correspond to the drag force during transverse particle motion, the force of particle inertia, the Saffman force associated with the gradient of the average gas velocity, the electrostatic repulsive force, forces of a radiometric nature (thermo- and photophoresis), and the effect of particle migration in an inhomogeneous pulsating velocity field. Moreover, some effects (considered in [13, 14], for example), whose contribution for the particles under consideration $d_s < 10 \mu$ is known to be small according to estimates made, are not included in (2). The boundary conditions for the system (1), (2) follow from the condition of stream symmetry along the axis ($R = 0$):

$$\begin{aligned} V_s = 0; \quad \frac{dU_s}{dR} - \frac{dU}{dR} = 0; \\ U_s = U(0) - Fr Stk (1 - \rho/\rho_s) - 4\psi Stk V_\tau^2, \quad (3) \end{aligned}$$

where the coefficient ψ takes account of the difference between the turbulent viscosity of a gas ν^* and the particle coefficient of turbulent diffusion D_S . Information about the radial distribution of the fundamental turbulent flow characteristics of a carrying medium is needed in addition to the boundary conditions (3) in order to analyze the system of motion equations (1), (2). An analysis of data in the literature [15-17] permitted setting up the following dependences on the dimensionless distance from the wall $y \equiv 0.5 V_\tau Re(1-R)$:

a) for a viscous, near-wall layer ($y < 7.8$)

$$U = V_\tau \left[1.98 \ln \left| 1 + \frac{35.6y}{141 - 11.85y + y^2} \right| + 6.85 \arctg \frac{y - 5.93}{10.3} + 3.58 \right], \quad (4)$$

$$\varepsilon = v^*/v \simeq 6 \cdot 10^{-4} y^3, \quad (5)$$

$$\langle V'^2 \rangle = V_\tau^2 \left(\frac{y}{6 + y} \right)^4; \quad V_\tau \simeq 0.168 \text{Re}^{-1/8}; \quad (6)$$

b) for the flow core ($y > 7.8$)

$$U = V_\tau \left\{ \frac{1}{0.39} \ln \left[1 + 0.39(y - 7.07) \right] + 6.68 + \frac{1}{12.6} \ln(0.03 + 0.97R) \right\}, \quad (7)$$

$$\varepsilon \simeq 0.39(y - 7.07)(0.03 + 0.97R), \quad (8)$$

$$\langle V'^2 \rangle = V_\tau^2 [0.78 + 0.22 \cos \pi(1 - 1.25R)]. \quad (9)$$

Hence

$$\frac{dU}{dR} = - \frac{1}{2} \text{Re} V_\tau R / (1 + v^*/v) \quad (10)$$

in each of the zones. The dependences (4)-(9) differ somewhat from the standard in connection with the need to comply with the continuity conditions of the field U , ε , dU/dR , $\langle V'^2 \rangle$ on the boundary of the near-wall layer. The expressions (6) and (9) have been obtained by approximating the data presented in [15, 16]. Since the particle concentration in the stream is considered sufficiently small ($\beta < 10^{-4}$), the dependences (4)-(9) obtained for the gas stream can be used to furnish the characteristics of a carrying medium.

For a numerical solution the initial system of differential equations (1)-(2) is replaced by a system of finite-difference equations of interpolation type. The channel radius is divided into three integration intervals and the spacing is diminished with the growth in the radial coordinate during passage from one interval to another. This permitted taking account of the sharp change in all functions in the area of the viscous boundary layer and an essential diminution in the volume of computational work without significant accumulation of computational error. Values of the desired functions at two initial nodes of the mesh follow from the boundary conditions (3). The exception is the value of $V_S(h_1)$. It is calculated from the second equation of the system by using an Euler interpolation formula. To obtain values of the desired functions at each next node of the mesh, the solution of the appropriate nonlinear algebraic system is performed by a Zeidel-type iteration method. Values calculated at the preceding mode are taken as initial approximations. The iteration process turned out to converge rapidly. It turned out to be sufficient to perform not more than six iterations to obtain a solution of the system to 10^{-8} accuracy at any node of the mesh. A change in the integration spacing during the passage from one range to another required an additional calculation of the missing values of the function $U_S(R)$ near the boundaries of the intervals. To do this, linear interpolation of the slowly varying function $U(R) - U_S(R)$ was performed. An M-220 electronic digital computer was used for the numerical solution of the problem.

The axial and radial particle velocities in a turbulent gas suspension stream were computed by the method presented above for $D = 0.1-1$ m; $u_0 = 1-10$ m/sec; $d_S = 0.1-1$ μ ; $\beta \rho_S / \rho = 10^{-2}-10^0$; $q_1 = 10^{-6}-10^{-4}$ C/kg. This determined a broad range of changes in the criteria Re , Fr , Stk , Bi_R , Sc , Bu , K_E . For definiteness in the numerical analysis, an air stream ($P = 1$ atm and $T = 300^\circ\text{K}$) was considered with graphite particles ($\rho_S / \rho = 1.35 \cdot 10^3$). The optical properties of the particles were determined according to [18]. The stream temperature mode was given by the condition $T_W / T_0 = 0.8-1.2$, i.e., the temperature drops were slight. Characteristic for the d_S values under consideration is $\psi = 1$, and the smallness of the particle concentration permits the hope that the first approximation in $\beta \simeq \text{const}$ will be correct. The computation results were compared for the developed turbulent mode.

In order to comprehend the causes predetermining any character of the transverse particle velocity profile, it is expedient to compare the magnitudes of the forces obtained in the numerical solution. In addition to the influence of the dimensionless factors, the influence of the initial dimensional quantities which enter simultaneously in several criteria can also be traced. Examples of the radial distributions of the forces governing the local values of the transverse particle velocity V_S are represented in Fig. 1a-d. The curves in this figure correspond to dimensionless quantities which are defined by the ratio between the local value

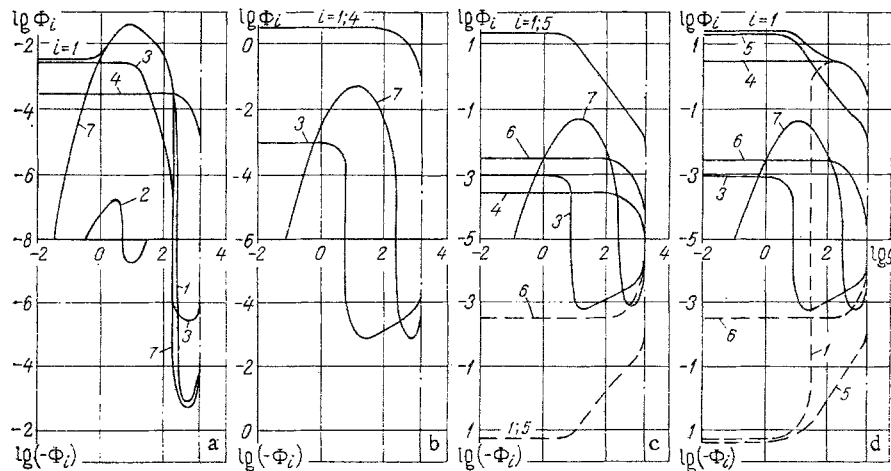


Fig. 1. Radial distributions of the forces acting on a particle: $Re = 6.2 \cdot 10^4$; $Sc_m = 3.3 \cdot 10^5$; $Bi_R = 10^{-8}$; a) $Fr = 9.8 \cdot 10^{-3}$; $Stk = 0.465 \cdot 10^{-3}$; $Bu = 0.167$; $D/d_S = 10^5$; $K_E = 3.25 \cdot 10^{-4}$; $T_w/T_0 = 1.0$; b, c, d) $Fr = 9.8$; $Stk = 0.465 \cdot 10^{-5}$; $Bu = 1.67$; $D/d_S = 10^6$; c) $K_E = 3.25 \cdot 10^{-4}$; b and d) $K_E = 3.25$; for c and d the solid curves are for $T_w/T_0 = 0.9$ and the dashed curves, for 1.1.

of some given force F_i and the scale of the stream inertial force estimated by means of the selected velocity and length scales: $\Phi_i = F_i r_w / \rho_S u_0^2$. In such form the quantities Φ_i correspond completely to the members in (2), and the subscript i corresponds to the sequence of writing the forces in this equation.

The drag Φ_1 equilibrates all the remaining forces acting on a particle in the radial direction. Hence, it is expedient to analyze the nature of its change along the radius on the basis of data about the distribution of the remaining forces. For the conditions taken it is obtained that the magnitude of the particle inertial force Φ_2 is negligible in all the versions. Its qualitative changes are hence observed: a change in sign during passage through the boundary of the viscous sublayer, the presence of extrema on both sides of this boundary, and the smooth reduction in absolute value of Φ_2 with recession from the extrema (Fig. 1a). Therefore, the numerical computation indicates the admissibility of neglecting the quantity Φ_2 in the range of parameters considered.

According to Fig. 1a-d, the magnitude of the Saffman force Φ_3 turns out to be negative near the stream axis for all the cases considered, decreases to the extremal point with the growth of R , and then rises abruptly and asymptotically approaches a positive constant value characteristic for the viscous sublayer. The relationship between the negative and positive sections of the curve hence depends on the comparable quantities $(U_S - U)$ and $(d_S/2)(dU/dr)$. Indeed, the first quantity predominates in the stream core, being negative in this region because of gravitational slip, but the second is positive and predominates in the near-wall layer where an abrupt change in velocity occurs. A diminution in the particular diameter, and even more so in the channel diameter (i.e., a reduction in the Stokes and Froude numbers), will result (Fig. 1a) in a diminution in the negative section and a magnification of the positive section of the curve $\Phi_3(R)$ since it is related, respectively, to the reduction in the contribution of gravity and to the origination of the inequality $U_S > U$ in the peripheral zone, which is due to predominance of the convective and diffusion transport of a longitudinal pulse under the influence of gravitation.

In contrast to Φ_3 , the magnitude of the particle electrostatic repulsive force Φ_4 does not alter the nature of the dependence on R as the flow parameters vary. The form of the dependence is determined by the monotonic change in the integral factor, but the variable parameters in K_E govern just the absolute value of the force. In conformity with the expression of K_E , a two-order-of-magnitude increase in the specific charge q_1 (from 10^{-6} to 10^{-4} C/kg) results in a four-order increase in Φ_4 . Exactly the same result is obtained also for an order-of-magnitude increase in the channel diameter if the condition $Re = idem$ is hence satisfied. Consequently, the electrostatic repulsive force greatly governs the transverse particle motion (Fig. 1b) for a fully realistic particle charge $q_1 = 10^{-4}$ C/kg for

large-diameter channels (for example, $D = 1$ m). A similar effect can be achieved for channels of lesser diameter only with an essential increase in the concentration, since $\Phi_4 \sim \beta$. The presence of particle electrostatic charges plays practically no part (Fig. 1a) for concentrations $\beta \sim 10^{-5}$ and $D = 0.1$ m. Therefore, a certain change in the initial data can transfer the magnitude of the force Φ_4 from the dominant to the negligible.

The thermophoresis force Φ_5 , turns out to be predominant in many cases even for a weakly nonisothermal stream, according to the results of the numerical solutions performed. Thus, for example, the thermophoresis force in the particular case $D = 1$ m, $q_1 = 10^{-6}$ C/kg determines the transverse particle velocity completely even for $|T_0 - T_w| \approx 10^{-3} T_0$, i.e., when the temperature drop between the wall and the stream is quite small: $\Delta T = 0.3^\circ\text{K}$. Only for an ideally nonisothermal flow can the thermophoresis force not be taken into account. The magnitude of the thermophoresis force depends strongly on the ratio of the diameter, since $\Phi_5 \sim (D/d_s)^2$. For the case $D = 1$ m, $d_s = 0.1 \mu$, even for an almost maximal particle charge, Φ_5 turns out to be predominant if the temperature head is at least several degrees. The change in Φ_5 along the radius agrees with the behavior of the velocity gradient curve: the thermophoresis force grows in absolute value (its sign is determined by the sign of the difference $T_0 - T_w$) with distance from the channel axis, reaches its maximum value at the boundary of the viscous layer, and does not change with a further approach toward the wall (Fig. 1c).

The nature of the change in the photophoresis force $\Phi_6(R)$ corresponds completely to the distribution of the force Φ_4 over the channel radius: a substantial growth in the flow core with distance from the channel axis and practical invariance starting already at $R \approx 0.8$. However, the photophoresis force Φ_6 turns out to be a comparatively small quantity in practice in all the cases considered, since the radiative heat fluxes were considerably less than the convective fluxes. Such a deduction agrees with [10]. However, a significant rise in the radiation criterion Bi_R (proportional to T^3) occurs with the rise in temperature and photophoresis can turn out to be the governing factor for high-temperature units. In this case, the dependence of Φ_6 on the particle and channel diameters can turn out to be important: Φ_6 changes in proportion to D^3 (for $Re = idem$) and is inversely proportional to d_s^2 . The simple D/d_s hence enters in the expression for the Bouguer criterion also, in which the magnitude of the absorption coefficient grows with the increase in d_s . The growth of the criterion Bu , due to the change in diameter or the increase in particle concentration, results in an increase in the quantity Φ_6 , and the dependence of Φ_6 on the radius becomes considerably steeper. At ordinary temperatures, thermophoresis is much more essential than photophoresis.

Besides the forces considered, the quantity Φ_7 , associated with the inhomogeneity of the pulsating velocity field of the carrying medium in the transverse direction, enters into Eq. (2) for V_s . If $\langle V_s'^2 \rangle = \langle V'^2 \rangle / (1 + Stk^2)$, then the magnitude of this force is determined only by the value of the Stokes criterion and the regularity of the change in intensity of the radial pulsations of the carrying medium. Only the second factor turns out to be governing in the range of conditions considered, since $Stk^2 \ll 1$ and does not influence Φ_7 in practice. The character of the change in Φ_7 in the cross section for $Re = idem$ (Fig. 1a-d) is practically independent of the stream parameters. The quantity Φ_7 diminishes from the zero value on the axis as R grows, passes through a minimum in the area of $R \approx 0.4$, and starts to grow monotonically, becoming positive at $R \approx 0.8$. Therefore, the migration mechanism results in particle motion toward the axis in the central part of the channel and toward the wall in the peripheral zone. A monotonic growth of Φ_7 is observed up to the viscous layer boundary. For $y = 10$ the function has a maximum whose magnitude exceeds the value of the minimum at $R \approx 0.4$ almost 40-fold, and Φ_7 is sharply reduced with a further approach to the wall. Let us note that in contrast to [12], the maximum of Φ_7 holds not for $y = 1$, i.e., not in the depth of the viscous layer in direct proximity to the wall, but for $y \approx 10$, i.e., on the outer boundary of the near-wall layer. Hence, the invalidity of the deduction [12] that Φ_7 is the single reason for particle precipitation follows. Computations show (Fig. 1a) that even in those few cases when the migration component predominates over the remaining members in (2) on a major part of the stream cross section, this relationship is spoiled near the wall because of the sharp drop in Φ_7 , and the forces for which the asymptotic tendency to some constant value as $y \rightarrow 0$ (for instance, $\Phi_3 - \Phi_6$) become governing.

The combined effect of all the forces considered affects the formation (because of the predominant factors) of the characteristic drag distribution Φ_1 . Curves not of Φ_1 but of $-\Phi_1$, which correspond completely to typical profiles of the transverse average particle velocity because of $V_s = -\Phi_1 / Stk$, are represented in Fig. 1a-d, for the sake of clarity. Four groups of such diagrams hence are produced on the basis of the numerical solution. The first

is represented in Fig. 1b for a predominant electrostatic force. The second (Fig. 1c) corresponds to the case when the thermophoresis force predominates. The thermophoresis and electrostatic forces are commensurate for the third group (Fig. 1d) and predominate over the remaining effects. The solid lines in Fig. 1c and d correspond to the case when the radiometric forces ϕ_5 and ϕ_6 are positive and the dashed curve, to when they are negative. For positive thermophoresis this results in a nonmonotonic behavior of the curve of ϕ_1 or $V_S(R)$, respectively, as compared with Fig. 1c because of the sharper growth in V_S in the central part of the stream (Fig. 1d). Hence $V_S > 0$ in the whole domain. If the sign of the thermophoresis force is negative, then particles on both sides move toward the point $R \approx 0.96$ from which they should spread out over the section because of the diffusion mechanism. In the case of the fourth group (Fig. 1a), the Saffman forces and the migration component are governing. Near the axis the quantity V_S changes sign upon imposition of positive thermophoresis, and V_S is positive in the rest of the domain. Hence, ϕ_7 predominates in the area of $y \approx 10$, but thermophoresis becomes governing for small y . If the thermophoresis force has a negative sign, then the profile $V_S(R)$ is determined by the opposition of the two mechanisms mentioned. The effects of migration ϕ_7 and the Saffman force ϕ_3 become the principal factors for an isothermal stream (in the absence of radiometric forces). The first of these factors governs practically the whole $V_S(R)$ field, while the second predominates in the near-wall zone (Fig. 1a). The sign-variability of the profile is such that particles move to the wall and to the axis from the section $R \approx 0.8$.

The analysis of the numerical solution performed shows that the magnitude of the particle radial velocity and the nature of its dependence on the radius vary substantially even for a quite insignificant change in the initial flow parameters. It can therefore be asserted that each of the papers [4-12], which rely only on some particle transport mechanism, can be valid only in some strictly bounded range of the dimensionless parameters in the initial system of equations. The present computations of U_S and V_S , performed in the considered range of initial characteristics, show that the most distinct quantitative and qualitative effects can appear depending on the interaction between the different transport mechanisms for a different relationship between the magnitudes of the forces. It is evident that real physical conditions, when the factors which exerted no significant influence in the range considered (the Saffman force, particle inertia, photophoresis, etc.) can affect the flow picture substantially, are completely possible.

The initial dependences, as well as the methodology of the numerical solution developed and realized for particular conditions, permit performing an analysis also for other cases not considered in this paper. The information about the particle behavior in a carrying stream which has been obtained can be used to study a concentration field of particles, their interaction with the channel walls, and to solve other related problems.

NOTATION

D, d , channel and particle diameters; D_S , coefficient of particle diffusion; k_f , radiation absorption coefficient of particles; r, x , radial and longitudinal coordinates; T , temperature; u, v , longitudinal and transverse velocities; v_T , dynamic velocity; $(\langle v'^2 \rangle)^{1/2}$, root-mean-square velocity pulsation in the radial direction; β , volumetric particle concentration in the stream; λ , coefficient of thermal conductivity; ν, ν^* , coefficients of molecular and molar viscosity; ρ , density; σ , Stefan-Boltzmann constant. Indices: 0, value of quantities on the stream axis; s, solid particles; w, value on the channel wall.

LITERATURE CITED

1. Z. R. Gorbis, Heat Exchange and Hydromechanics of Through Streams [in Russian], Énergiya, Moscow (1970).
2. Z. R. Gorbis and F. E. Spokoinyi, Inzh.-Fiz. Zh., 15, No. 4 (1968).
3. P. Zenker, Staub, 32, 1 (1972).
4. N. N. Kondič, Trans. ASME, 92C, 117 (1970).
5. R. S. Prasolov, Mass and Heat Transfer in Furnaces [in Russian], Énergiya, Moscow-Leningrad (1964).
6. W. Walkenhorst, Aerosol Sci., 1, 225 (1970).
7. S. L. Soo, in: International Reviews in Aerosol Physics and Chemistry, Vol. 2, Pergamon Press (1971).
8. S. L. Soo and S. K. Tung, Powder Technol., 6, 283 (1972).
9. P. O. Rouhiainen and J. W. Stachiewicz, Trans. ASME, 92C, 118 (1970).

10. A. I. Leont'ev and É. A. Tsalko, Heat and Mass Transfer in Disperse Systems [in Russian], Vol. 2, Naukova Dumka (1972).
11. C. Wakstein, Aerosol Sci., 1, 69 (1970).
12. E. P. Mednikov, Dokl. Akad. Nauk SSSR, 203, 543 (1972).
13. V. V. Orlov, Inzh.-Fiz. Zh., 19, 341 (1970).
14. F. A. Morrison, I. E. C. Fundam., 8, 594 (1969).
15. J. O. Hinze, Turbulence, McGraw-Hill (1959).
16. J. Comte-Bellot, Turbulent Flow in a Channel with Parallel Walls [Russian translation], Mir, Moscow (1968).
17. M. D. Millionshchikov, Turbulent Flows in Boundary Layers and Pipes [in Russian], Moscow (1969).
18. A. G. Blokh, Thermal Radiation in Boilers [in Russian], Énergiya, Leningrad (1967).
19. Z. R. Gorbis and F. E. Spokoinyi, Izv. Akad. Nauk SSSR, Mekh. Zhidk. Gaza, No. 1 (1969).

FORMATION OF A GAS BUBBLE ON A VIBRATING CAPILLARY

IMMERSED IN A LIQUID

I. S. Grachev, D. T. Kokorev,*
and V. F. Yudaev

UDC 532.529.6

The formation of a train of bubbles in a low-viscosity liquid is investigated. The dependence of the gas flow rate during formation of the bubble train on the vibrational acceleration of the capillary is determined.

One of the techniques used to intensify mass transfer at a liquid-gas or liquid-liquid interface is to disperse one of the phases by means of a vibrating nozzle or macrocapillary (bubbling, dispersion, etc.). This technique enables one to control the particle size of the dispersed phase over a wide range and to increase the relative velocity of the interacting phases. In the present study we attempt to formulate a fluid-mechanical description of the formation of a single gas bubble on a vibrating macrocapillary immersed in a liquid.

To derive the bubble-growth equation we assume that: 1) the surface-tension forces impart a spherical shape to the bubble; 2) prior to breakoff the bubble remains rigidly connected to the capillary, which vibrates in a vertical plane according to a harmonic law. In the direction of the vertical axis, therefore, the center of the growing bubble is simultaneously involved in two motions, one reciprocating $A \sin \omega t$ and the other translational $R(t)$ due to its own growth (Fig. 1a), such that

$$z = R(t) + A \sin \omega t. \quad (1)$$

The velocity of the center of the bubble is

$$U = \frac{dz}{dt} = \frac{dR}{dt} + A\omega \cos \omega t. \quad (2)$$

The velocity potential of the liquid surrounding the growing spherical bubble is written as follows [1]:

*Deceased.

Moscow Institute of Chemical Machinery. Translated from Inzhenerno-Fizicheskii Zhurnal, Vol. 30, No. 4, pp. 665-670, April, 1976. Original article submitted March, 5, 1973.

This material is protected by copyright registered in the name of Plenum Publishing Corporation, 227 West 17th Street, New York, N. Y. 10011. No part of this publication may be reproduced, stored in a retrieval system, or transmitted, in any form or by any means, electronic, mechanical, photocopying, microfilming, recording or otherwise, without written permission of the publisher. A copy of this article is available from the publisher for \$7.50.